JOURNAL OF CATALYSIS 91, 231–240 (1985)

Silica-Supported Iron Nitride in Fischer–Tropsch Reactions

I. Characterization of the Catalyst

E. YEH,* N. K. JAGGI,* J. B. BUTT,† AND L. H. SCHWARTZ*

*Department of Materials Science and Engineering and †Department of Chemical Engineering, Ipatieff Laboratory, Northwestern University, Evanston, Illinois 60201

Received September 1, 1983; revised April 30, 1984

The techniques of Mössbauer effect spectroscopy and wide angle X-ray diffraction have been applied to characterize nitrided iron catalysts (initial composition $\approx Fe_2N$) supported on silica gel and used in the synthesis reaction. Mössbauer spectroscopy shows that the nitride catalyst becomes iron-rich during the first 3 h of reaction in the syngas environment ($CO:H_2 = 1:3$, $T =$ 250°C, 7.8 atm) indicating that nitrogen atoms are removed more rapidly by H_2 than they are simultaneously replaced by carbon atoms. After 3 h carburization becomes dominant, the carbon concentration increases, and the catalyst composition stabilizes after about 18 h of reaction. The analysis of the 4.2 K Mössbauer spectrum and X-ray diffraction of an equilibrated catalyst after 49 h of reaction gives a composition of $Fe_{2.18}C_{1-y}N_y$, where y was estimated to be between 0.13 and 0.20.

INTRODUCTION

In the 1950's nitrided iron catalysts for the Fischer–Tropsch reaction were developed at the Bureau of Mines (*1–3*). Since then, a few studies of the iron nitride catalyst have appeared elsewhere (*4–5*). All the reported iron nitride catalysts were either in the precipitated or fused forms with ingredients such as CuO, K_2O, Al_2O_3, MgO, and SiO_2 as promoters. One significant feature of the reported behavior of the iron nitride catalyst is high alcohol selectivity. In the present study, a silica-supported, fine-particle (~10 nm) iron nitride catalyst has been investigated without any promoter in order to sudy the effect of the presence of nitrogen atoms in the catalyst. Mössbauer effect spectroscopy (MES) and wide-angle X-ray diffraction (XRD) were used to characterize the catalyst prior to and after various times of reaction and these characterizations are reported here.

If we write the composition of the catalyst as $Fe_x(C_{1-y}N_y)$, then one is interested in the variation of y and x with time on stream.

In the accompanying paper, Part II, the reaction studies of the supported iron nitride catalyst with and without potassium promotion will be reported and a comparison will be made between the effects of potassium and nitrogen.

Earlier work on kinetics of nitrogen removal from fused nitride catalysts (*3*) is of little help in deciding the rate of removal/replacement of nitrogen from the ~10-nm nitride particles used in the present study. Diffusion data for nitrogen in the ε-phase are not available, but we can use the value of the interstitial diffusion coefficient in a close-packed iron lattice at 200°C, i.e., 10^{-16} cm²/sec as a good estimate. Using $\sqrt{Dt}$ as the measure of diffusion length, we find $t \approx 1$ h for a diffusion length of 5 nm (~ half the particle diameter). Thus unrestricted interstitial diffusion would deplete all the nitrogen in a time frame of hours. While the activity–selectivity data of the nitride catalyst (Part II) was found to approach that of the carbide catalyst, in a comparable time frame, substantial differences remained after 2 days. It is thus im-

0021-9517/85 $3.00

portant to determine how much nitrogen, if any at all, persists in the catalyst under reaction conditions. The much longer time scale of nitrogen removal in fused bulk catalysts (*3*) is easily understood because diffusion time varies as the square of the distance over which the particle has to diffuse.

EXPERIMENTAL

Sample preparation. The samples were prepared by impregnating Davison Grade 62 silica gel (80/120 mesh) with an aqueous solution of $Fe(NO_3)_3$ to incipient wetness; the loading was 9.8 wt% based on iron metal. After the samples were dried at 125°C overnight they were calcined in air at 200°C for 2 h and then at 450°C for 4 h. For comparison with previous work, a portion of the calcined iron was reduced at 425°C for 24 h with flowing H_2 prior to use in a Fischer–Tropsch reaction. This sample quickly carburized in the syngas reaction at 250°C and will be designated "Fe-carbide" hereafter. The nitride catalyst (hereafter "Fe-nitride") was prepared by passing NH_3 through the catalyst bed for 12 h at 495°C after 24 h of reduction in H_2 at 425°C.

Mössbauer spectra. Spectra were obtained with a spectrometer operated in "fly back" mode using ^{57}Co in Rh foil as the source. Spectra were fitted using a standard least-square routine in a constrained manner. Isomer shfits (*IS*) are reported with respect to iron metal.

X-Ray diffraction. X-Ray measurements were made using a CoK_α radiation source. In all cases an iron filter was employed to reduce the K_β X-ray intensity. All data were accumulated in a point-counting mode to improve the statistical accuracy in peak locations and lineshapes. Particle size estimates were made using the Scherrer method.

RESULTS

Room-temperature Mössbauer spectra of the catalyst after 0, 0.5, 3, 18, and 49 h of reaction are shown in Figs. 1A, B, C, 2A, and B, respectively. The spectra for 18 and 49 h of reaction are virtually identical, so one of them (49 h) was run at 4.2 K to completely characterize the composition of the used catalyst. This spectrum is shown in Fig. 2C.

The X-ray diffraction profiles for the Fe-carbide (3 h in synthesis reaction) and Fe-nitride (before use) are shown in Figs. 3A and B, respectively. The results for the remaining samples are summarized in Table 1.

DISCUSSION

Nitride Catalyst at t = 0

The structure of iron nitride has been studied quite extensively (*6, 7*). Bainbridge *et al.* (*8*) prepared iron nitride by flowing ammonia over thin iron foils at 486°C for 50 h and obtained orthorhombic ζ-Fe_2N as confirmed by X-ray analysis. In the present

TABLE 1

Summary of X-Ray Measurements as a Function of Time in the Syngas Environment (λ (CoK_α) = 1.7903 Å)

Time (h) Fe-nitride	2θ (002)	d (002) (Å)	2θ ($1\bar{1}1$),(101)	d ($1\bar{1}1$),(101) (Å)	c (Å)	a (Å)	c/a	FWHM(101)
0	47.9	2.205	50.4	2.102	4.410	2.761	1.597	0.9
1/2	48.2	2.192	51.0	2.079	4.384	2.727	1.608	1.05
3	48.5	2.179	51.4	2.064	4.358	2.706	1.610	1.05
18	48.3	2.188	50.4	2.102	4.376	2.767	1.581	0.9
Fe-carbide								
3	48.5	2.179	49.8,50.4	2.125,2.103	4.358	2.773	1.572	

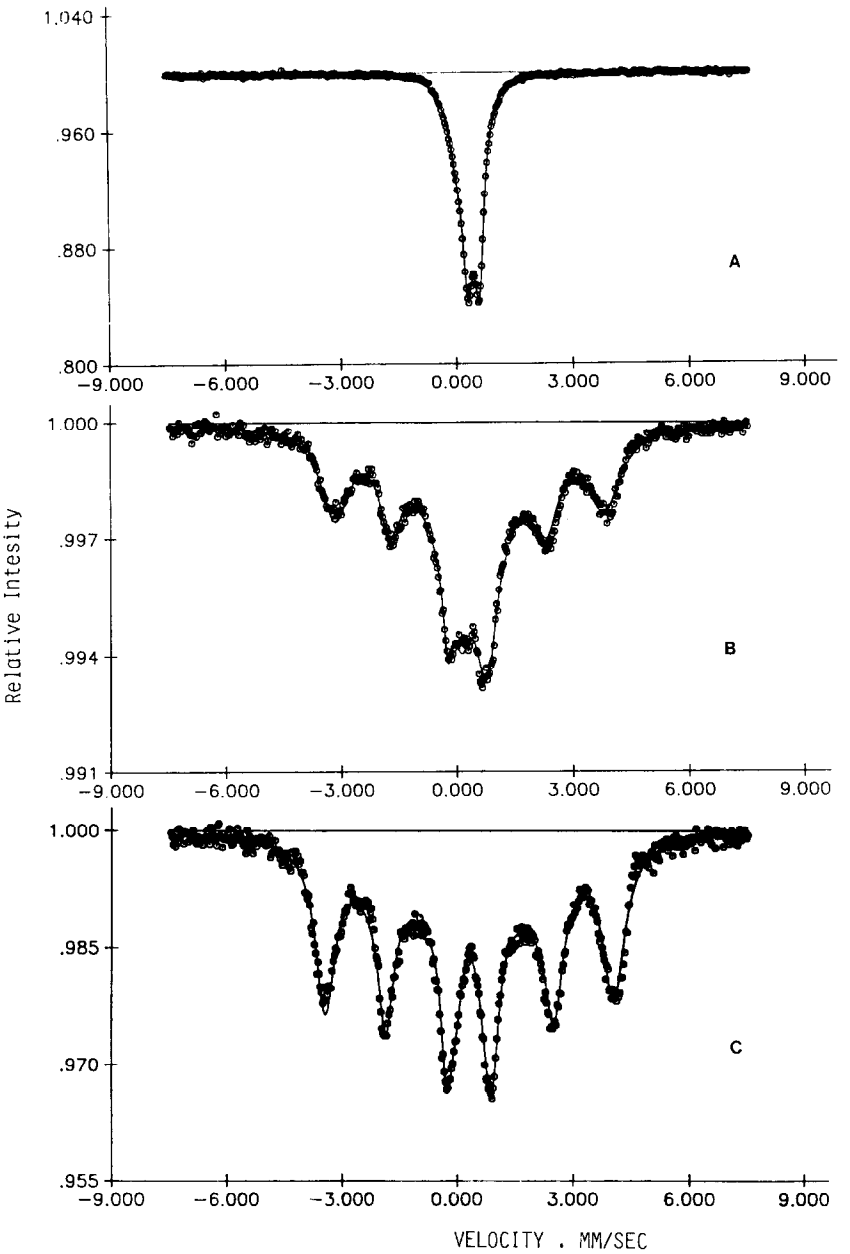

FIG. 1. Room-temperature Mössbauer spectra of Fe-nitride catalyst after (A) 0 h, (B) 0.5 h, (C) 3 h in synthesis reaction.

study, the nitridation period was 12 h. Chen *et al.* (*9*) prepared iron nitride from unsupported iron powder using the same procedure as in the present study and obtained a composition of $Fe_{2.08}N$. If the supported iron behaves the same way as an unsupported sample, then the starting catalyst is in the ε-phase with an Fe/N ratio slightly higher than 2, consistent with the X-ray diffraction result. The parameters for the quadrupole doublet are almost identical to the reported values for ε-$Fe_{2.08}N$ (*9*), however

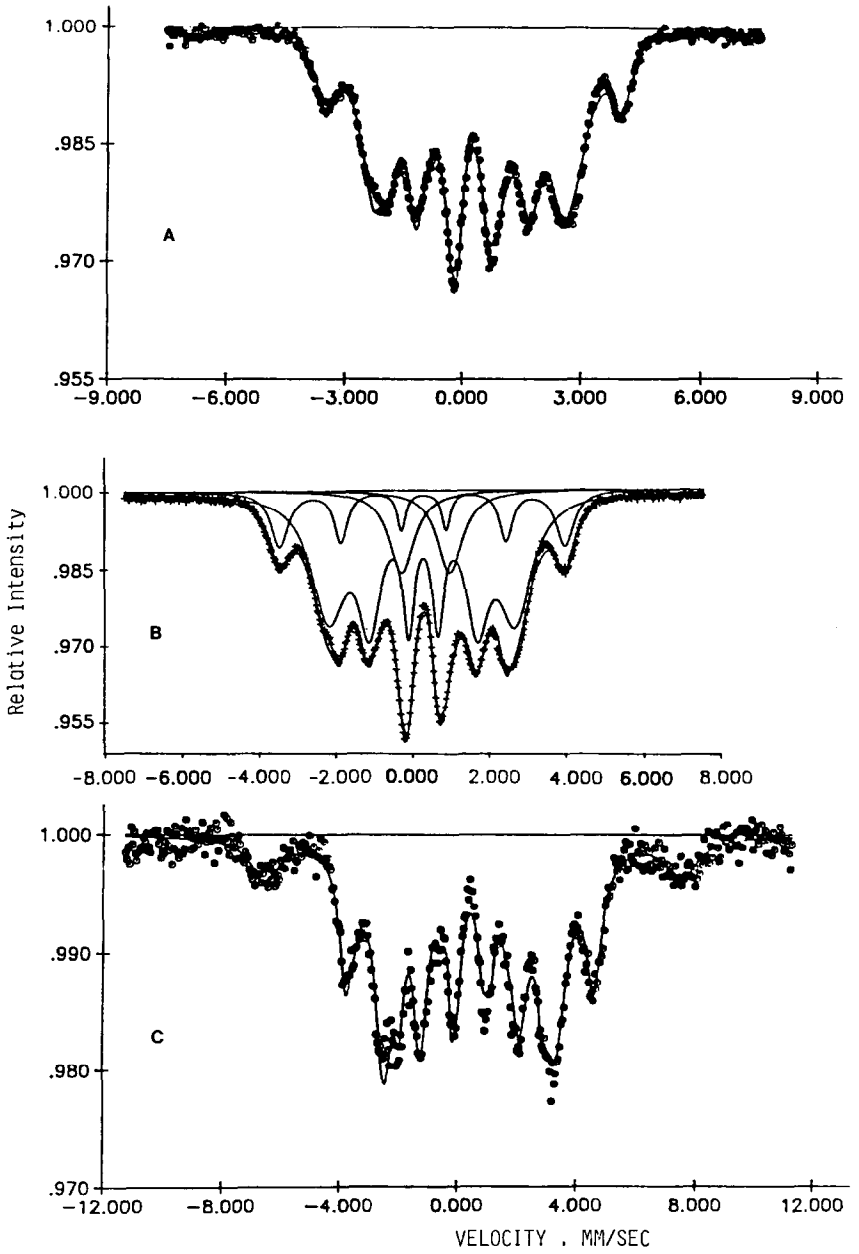

FIG. 2. Room-temperature Mössbauer spectra of Fe-nitride catalyst after (A) 18 h and (B) 49 h in synthesis reaction. The liquid-He spectrum of 49-h sample is shown in (C).

the spectrum cannot be fitted to just one doublet because of a broad structure in the wings. An excellent fit is obtained if one includes a second doublet. The larger *QS* for the second doublet is probably from the iron atoms with two nitrogen nearest neighbors which must be present for $x > 2$ in Fe_xN.

Particle sizes of the calcined and reduced iron catalyst supported on SiO_2 have been measured by Amelse *et al.* (*12*). However, determining the particle size for supported

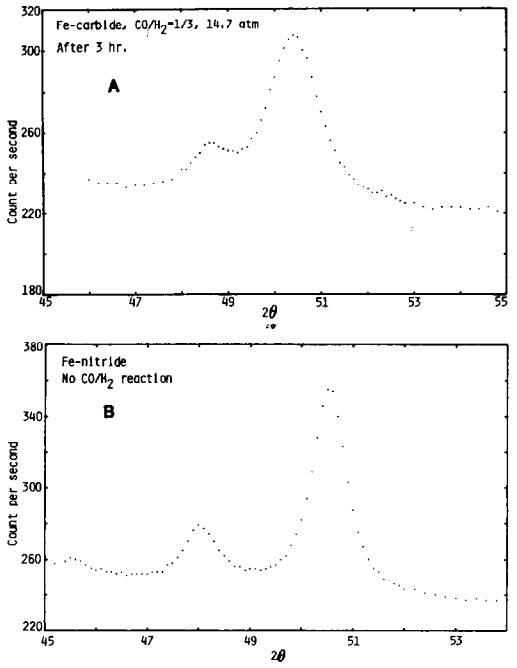

FIG. 3. X-Ray diffraction intensity vs 2θ for (A) Fe-carbide catalyst after 3 h in syngas mixture, (B) Fe-nitride catalyst before synthesis reaction.

iron carbide and iron nitride catalyst by X-ray lineshape analysis is prohibited by the complexity of the peak profiles which makes deconvolution of individual diffraction peaks highly unreliable. Thus no attempt was made to measure the absolute dimensions of the carbide and nitride particles in this study. It was possible, however, to make useful comparisons of relative sizes.

The less-intense peak at about 48.0° is indexed as the (002) reflection for the hexagonal unit cell appropriate for the ε-phase. The more intense peak at about 50.5° is ascribed to the superposition of $(1\bar{1}1)$ and (101) peaks, which would be degenerate for a regular HCP structure. Any distortion from the HCP structure would split this peak: e.g., for orthorhombic ζ-Fe_2N, Bainbridge *et al.* (*8*) found two peaks at 40.1° and 50.4° corresponding to the (021) and (211) peaks indexed according to the orthorhombic unit cell.

In any case, the full width at half maximum (FWHM) for the (002) peak is about 1.1° for both carbide and nitride catalysts, indicating an approximate equality of average particle sizes for the two materials, which is about 10 nm. The apparently larger broadening of the 50.5° peak of the Fe-carbide catalyst is presumably due to the splitting of the $(1\bar{1}1)$ and (101) peaks due to a slight distortion of the HCP unit cell, as has been reported by Barton and Gale (*13*), that remain unresolved due to the small particle size in the present study. A qualitative examination of the Fe-nitride catalyst before the syngas reaction using transmission electron microscopy (*14*) confirmed that neither the particle size nor morphology of the supported particles exhibited obvious differences from those of the Fe-carbide catalyst.

Composition of the Catalyst after 49 h of Reaction

The continued presence of nitrogen in the used catalyst was confirmed chemically by a decomposition method. When the sample was heated in flowing H_2 and held at 400°C for 4 h, the catalyst was reduced to give methane and ammonia as products which were trapped in a dry-ice–acetone bath. The presence of ammonia was detected by a thermal conductivity cell and also by precipitating brown $Fe(OH)_3$ from an aqueous solution of Fe^{3+}. Attempts at conventional chemical analysis for quantitative estimation of N, even for pure nitrides, were thwarted by the inability to distinguish between N that is adsorbed on the support and that which is present as Fe-nitride. It takes only a small amount of spurious nitrogen, given the low metal loading, to render the estimation of N content unreliable.

Therefore we have used the combination of Mössbauer and X-ray diffraction to estimate x and y and to identify the phases. The difficulties in using X-ray diffusion alone for phase analysis of fine particle carbides in the presence of a large amount of silica have been known for some time (*11*). Our Mössbauer spectra of the present used cat-

alyst cannot rule out the presence of small amounts of θ-Fe_3C, but the θ-carbide forms at much higher carburization temperature, e.g., 823 K (*20*) or 723 K (*11*) and was not indicated by our X-ray data. The presence of χ-phase along with ε-phase is difficult to detect by X-ray diffraction; however, the Mössbauer spectrum of χ-Fe_5C_2 has a distinct sextet with $HF \simeq 120$ kOe at room temperature. Since our spectra fit reasonably well without this sextet, we believe that the amount of χ-carbide is small, if any. Finally, the ternary-phase diagram (*22, 23*) of the Fe–N–C system at 500°C shows a very wide region of ε-Fe_x(NC) with large solubility for both types of interstitials. This ε-phase region is believed to be even wider at the lower temperatures we studied (*22, 23*). Since the starting catalyst is ε-$Fe_{2.08}N$, we therefore expect the material to stay in the ε-phase field even for large replacement of N by C. Our analysis that the material is mostly ε-Fe_x(NC) is consistent with the phase diagram and the known tendency of small particle size to stabilize hexagonal ε-carbide as opposed to monoclinic χ-carbide (*11*). The analysis of Mössbauer and X-ray data to obtain x and y, given in later sections, will implicitly assume that most of the material is in the ε-phase.

Characterization by Mössbauer Spectroscopy

The room-temperature Mössbauer spectrum was fit to two sextets and one broad quadrupole doublet (Fig. 2B). A distribution of hyperfine fields (*HF*) is apparent and the sextets were fit with the linewidths increasing linearly from the center (see Ref. (*9*)) of the spectrum with a slope "*S*." The value of *S* is a measure of the width of the distribution of *HF*, and was left as a free parameter for each sextet. This approximation does not account for the deviation of the lineshape from Lorenzian which results from the *HF* distribution. Consequently, there are small systematic misfits in the outermost lines. Since all the samples were thin and lightly pressed powders, the relative area ratios for the sextet were constrained to be 3 : 2 : 1 : 1 : 2 : 3. If the magnitude of the quadrupole splitting (*QS*) is small and the angle between the electric field gradient and the magnetic axis is fluctuating from site to site, as may be expected for ε-Fe_x(NC), one will get broadened, but symmetric, sextets. Indeed, the quality of the fit with *QS* as constrained to zero for the sextets was no different from that when *QS* was left as a free parameter, in which case the fitted value was close to zero. In the fits of the room-temperature spectra shown in Table 1, *QS* was constrained to be zero for the sextets. It should be noted that it was essential to include a broadened, nonmagnetic, quadrupole-split doublet in order to obtain good fits to the room-temperature spectra. The parameters of the fit are listed in Table 2. The nonmagnetic doublet splits into a Zeeman sextet at 4.2 K and the fit is shown in Fig. 2C.

The room-temperature value of isomer shift (*IS*) is 0.3 mm/sec and the liquid-He temperature value of $HF = 440$ kOe prove that this latter component is due to Fe^{3+} ions. The very large value of the (*QS*) of 1.1–1.3 mm/sec does not agree with any known crystalline oxides, hydroxides, or oxyhydroxides of iron. However, amorphous Fe_2O_3 has been prepared by sputtering (*15*) and has been found to have *HF* (4.2 K) = 460 kOe, *IS*(RT) = 0.3 mm/sec, and *QS*(RT) = 1.1 mm/sec. Similarly, a *QS* of about 1 mm/sec and an *HF* of about 450 kOe at 4.2 K have been reported (*16*) for Fe^{3+} in amorphous ferric oxide prepared by thermal decomposition of an aerosol. We therefore identify the doublet as coming from amorphous ferric oxide which explains why it is not observed in the X-ray diffraction even though it is present in significant amount. There is no known carbide of iron with such a large value of QS and therefore the doublet cannot be due to superparamagnetic carbide.

Physically, the two sextets *HF*(3*I*) and *HF*(2*I*) correspond to two sites in the same crystallographic phase with 3 or 2 intersti-

TABLE 2

Mössbauer Parameters and Identification of the Various Samples

Sample	*IS*/Fe (mm/sec)	*QS* (mm/sec)	*HF* (kG)	*I*/*I* Total (%)	Identity	Average composition
49 h	0.42 (±.05)	0.0 (±.2)	180 (±1)	61 ±2	Fe(3*I*)	
(liq.-He	0.43 (±.05)	0.1 (±.2)	261 (±1)	20 ±2	Fe(2*I*)	$x = 2.18$
Temp.)	0.49 (±.1)	0.0 (±.2)	438 (±4)	19 ±3	Amorp. Fe^{3+}	$y = 0.13$
49 h	0.27		152	66	Fe(3*I*)	
(*RT*)	0.28		231	16	Fe(2*I*)	$x = 2.18$
	0.34	1.3	0	18	Amorp. Fe^{3+}	
18 h	0.26		155	62	Fe(3*I*)	$x = 2.18$
(RT)	0.28		233	20	Fe(2*I*)	Almost the same as 49 h
	0.26	1.3	0	18	Amorp. Fe^{3+}	
3 h	0.23		140	50	Fe(3*I*)	$x = 2.52$
(RT)	0.31		233	35	Fe(2*I*)	$y = 0.56$
	0.29	1.1	0	15		"Slope" large. Therefore N/C inhomogeneous
0.5 h	0.41	0.52	0	19	Fe(3N)	Mixture of two phases with
(RT)	0.32		216	47	Fe(2N)	$x \simeq 2$, $y \simeq 1$, and $x \simeq 3$,
	0.35	1.35	0	34	Amorp. Fe^{3+}	$y \simeq 1$, respectively
0 h	0.44	0.31	0	70	Fe(3N)	
(RT)	0.27	0.50	0	30	Fe(2N)	
					+Amorp. Fe^{3+}	$2 < x < 2.15$; $y < 1$

Note. The uncertainty for room-temperature (RT) spectra are approximately ±0.05 and 0.1 mm/sec, 3 kG, and 4% for *IS*, *QS*, *HF*, and area fraction, respectively.

tial neighbors, respectively, and their *f*-fractions are expected to differ only by small amounts. It is noted from Table 2 that the area fractions for the three components of the spectrum are approximately the same at room- and liquid-helium temperatures. This is very different from the conclusion of Amelse *et al.* (*12*) that the *f*-fractions and therefore the relative areas of the various components change drastically between room- and liquid-helium temperatures. An examination of their room-temperature fit reveals that this is due to unphysical intensity ratios of the inner sextet and overconstraint of the parameter that determines the variation of linewidth with line position. It is clear from Table 2 that it is meaningful to use the area fractions measured at room temperature to get the relative amounts of the two kinds of iron atoms, Fe(3*I*) and Fe(2*I*), as will be done later for other samples.

In the ε-phase each Fe atom is surrounded by six interstitial positions, of which a maximum of three are occupied by N or C atoms. A large amount of work has been done on the iron carbides (*18*) and the saturation *HF* associated with Fe(3C) and Fe(2C) are measured to be 173 kOe (*10, 12, 17–20*) and 241 to 245 kG (*7*). The *HF*'s of Fe(3N) and Fe(2N) are strongly dependent on the temperature and the overall nitrogen content because the Curie temperature decreases rapidly with increasing N content (*24–27*). The saturation *HF* for $Fe_{2+x}N$ have been measured by Chen *et al.* (*9*). These values are listed in Table 3. Thus one ambiguously identifies the sextet with a field of about 235 kOe as originating in Fe(2*I*) atoms, where *I* could be a C or N atom. The other sextet with a smaller value of *HF* is then from Fe(3*I*), the actual value of *HF* depending upon composition. The value of x in $Fe_x(N_yC_{1-y})$ is immediately obtained by equating the number of Fe–I and I–Fe bonds as $x = 6/(2p_2 + 3p_3)$, where p_2 and p_3 are the fractions of Fe(2*I*) and Fe(3*I*) atoms. From the measured area ratios at 4.2 K for the 49-h sample we find $x = 2.18 \pm 0.03$. If the area fractions at room temperature are used, we get $x = 2.15$, in reasonable agreement with the 4.2 K result.

It is less straightforward to obtain the value of y. The saturation *HF* is known

TABLE 3

The Saturation Hyperfine Fields (SHF) Measured at 4.2 K for Fe(nI) (n = 2, 3; I = C, N) and Fe-nitride Catalyst after 49 h of Reaction

Fe(nI)	SHF (kOe)	Comment
Fe(3N)	65 < SHF < 140	Ave. = 100 kOe (*9*)
Fe(2N)	258	(*9*)
Fe(3C)	191	(*17*)
Fe(2C)	262	(*18, 19*)
Fe(3I) in Fe-nitride (49 h)	180	This work
Fe(2I) in Fe-nitride (49 h)	161	This work

only for pure Fe(3C) and Fe(3N) reliably, as approximately 191 and 100 kOe, respectively. Some work has been done on carbonitrides (*21*) but in view of ignoring the longer range effects on *HF* in the nitrides (see (*9*)) one cannot use those *HF* values in an obvious manner. In a simplistic manner, but the only meaningful way at present, we assume a linear variation of *HF*(3*I*) from the pure carbide to the pure nitride, and get $y = 0.13$ for the 49-h sample. Thus the composition of the stabilized catalyst after 49 h of reaction is $Fe_{2.18}(C_{0.87}N_{0.13})$.

The values of *IS*(2) for the carbonitrides (*21*) were found to be in the range of 0.28 to 0.32 mm/sec, compared to the values of 0.25 and 0.34 mm/sec for the carbide (*17–20*) and nitride, respectively (*21, 9*). These numbers have an uncertainty of 0.02 to 0.05 mm/sec. Therefore, they cannot be used to estimate the C/N ratio with any certainty. The measured *IS* for all our samples are consistent with the compositions deduced from the values of *HF*, which is a more sensitive measure of C/N ratio.

Mössbauer Spectra of the Catalyst at Intermediate Times

All the room temperature Mössbauer spectra have been fit the same way as the 49-h spectrum. These are shown in Figs. 1 and 2, while the important parameters are summarized in Table 2.

After 0.5 h of reaction the catalyst is a two-phase mixture (apart from the amorphous oxide). About 18% of the catalyst is present as nonmagnetic, nitrogen-rich material, corresponding to the quadrupole doublet with $QS = 0.5$ mm/sec. The composition of this component is $Fe_{2+y}N$ with $y < 0.2$, because at that value of y even pure nitride is magnetically ordered at room temperature. About 45% of the catalyst is present as an iron-rich, magnetic phase. The very small intensity of the *HF*(3*I*) suggests that this phase is close to the composition Fe_3N. The room-temperature values of *HF*(2C) in ε-$Fe_{2+x}C$, *HF*(2N) in Fe_3N, and *HF*(2N) in $Fe_{2.67}N$ are 242, 225, and 205 kOe, respectively (*9*). The significantly smaller value of *HF* = 216 kOe shows that this iron-rich phase is also carburized only to a small extent, if any. An analysis similar to that described above shows that after 3 h of reaction the nitrogen-rich nonmagnetic phase has vanished and one has an overall composition of approximately $Fe_{2.52}(C_{0.4}N_{0.6})$. Even though the extreme compositions corresponding to the nonmagnetic doublet are not present, the N/C ratio is inhomogeneous in this sample. This is suggested by the much larger FWHM and slope "*S*" for the 140-kG sextet in this sample than in the rest. The spectrum after 18 h of reaction is virtually identical to the 49-h spectrum. From the area ratios for the sextets corresponding to Fe(3*I*) and Fe(2*I*) at room temperature, one has $x = 2.16$ and the value of y is also close to that for the 49-h sample.

X-Ray Diffraction Patterns at Intermediate Times

Even though only two strong lines are detected in the diffraction pattern, one can obtain c,a and therefore c/a by indexing them with a hexagonal unit cell. Table 1 shows that the lattice parameters decrease for the first 3 h and then increase again. This can be due to either removal of N or replacement of N by C. Figure 4 is a plot of the c/a ratio for ε-nitride and carbides from

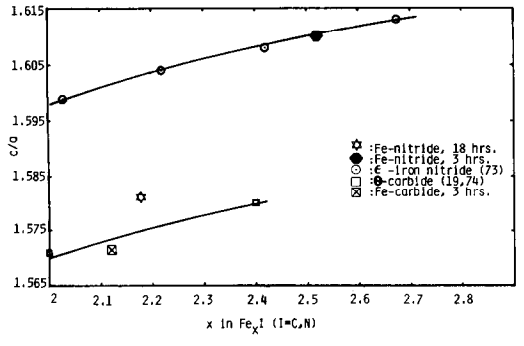

FIG. 4. The ratio c/a vs x in Fe_xI (I = C,N) for ε-iron nitride, iron carbide, and Fe-carbide, Fe-nitride after synthesis reaction.

the literature (*7, 13, 30*). The carbide with x = 2.12 in Fig. 4 is from the present study of the pure iron, carbided in the reaction mixture for 3 h, the value of x being obtained from Mössbauer spectroscopy as described earlier. It is clear that the points for the pure carbides and nitrides lie on two well-separated curves. Since x is now known, the experimentally determined c/a ratios can be used to estimate the C/N ratios to compare with the Mössbauer results.

The point for the 18-h reaction viz. x = 2.18 and c/a = 1.581 lies between the carbide and the nitride curves, a linear interpolation giving a value of y = 0.2, in reasonable agreement with the Mössbauer result.

It is obvious from the Mössbauer spectrum that the 0.5-h sample is a mixture of two phases: one relatively rich in nitrogen and the other relatively rich in iron. This is reflected in a slightly larger linewidth for the X-ray peaks as compared to the 0- and 18-h samples. The average value of x = 2.5 (obtained by weighting the compositions of the two phases with their relative amounts) and the c/a ratio of 1.608, when plotted on Fig. 4, show that carburization is negligible, in agreement with the Mössbauer result.

There is some discrepancy between the Mössbauer and X-ray analysis for the 3-h sample. The relatively large value of 140 kOe for average $HF(3I)$ proves that some carburization has certainly taken place: the linear extrapolation gives y = 0.6. However, the corresponding point for x = 2.52 and c/a = 1.610 on Fig. 4 suggests little carburization. Like the 0.5-h sample, the X-ray linewidths are slightly larger than for 0- and 18-h samples indicating the inhomogeneity of N/C ratio that was concluded from the Mössbauer spectrum. In view of the inability to deconvolute the X-ray peaks, we trust the Mössbauer result, viz. that some carburization has certainly taken place. Since the actual relation between $HF(3I)$ and N/C ratio is not well-known, the number y = 0.44 should be considered tentative.

SUMMARY AND CONCLUSIONS

With the reduced metallic iron catalyst, carburization is completed in 90 min, as has been reported earlier (*17*). However, the nitrided catalyst is not completely carburized even after 49 h. In fact the composition seems to stabilize after about 18 h to ε-$Fe_{2.18}(C_{1-y}N_y)$ where y is estimated to be between 0.13 and 0.20. This is consistent with the ternary-phase diagram of Fe–N–C (*22, 23*) which shows ε-Fe_x(NC) to have significant solubility for both types of interstitials. This single-phase region is even wider at 250°C (*22, 23*). The difference in kinetics of carburization are probably due to the different initial structure. The diffusion of C in bcc Fe is known to be rapid. However, in ε-Fe_xN, the strong interstitial repulsion will inhibit the diffusion of C or N through regions rich in Fe($3I$). At the starting composition of Fe_2N, since almost all the iron is present as Fe(3N), carburization is strongly diffusion-limited. As x increases with time due to removal of N atoms by H_2 (as has been observed by Mössbauer spectroscopy) carburization becomes more rapid. After 3 h, the average value of x is 2.52 and about 40% carburization has taken place. Thereafter, the catalyst composition shifts toward increasing C content, stabilizes at $Fe_{2.18}(C_{0.87}N_{0.13})$ after 18 h and does not change much thereafter.

The kinetics of N removal in the present study are fully consistent with the study of reduction of the carburized Fe catalyst of

comparable particle size by Raupp and Delgass (*29*). They found that 30% of the carburized catalyst was reduced to metallic iron after 10 h of reaction with flowing H_2 at 250°C, even though the initial carburization of bcc Fe was completed in about an hour. The much longer times of nitrogen removal replacement, observed in the earlier work on fused catalysts (1C) is understood in terms of their much larger particle size, but cannot be directly compared to the present results.

ACKNOWLEDGMENTS

This research was supported by the Department of Energy, Office of Basic Energy Sciences, Division of Materials Sciences, under Contract DE-AC02-78ER04993. Mössbauer and X-ray diffraction measurements were carried out at the facility laboratories of the Materials Research Center, Northwestern University.

REFERENCES

1. Anderson, R. B., *Catal. Rev.—Sci. Eng.* **21**(1), 53 (1980).
2. Anderson, R. B., "Advances in Catalysis," Vol. 5, p. 355. Academic Press, New York, 1953.
3. Hall, W. K., Dieter, W. E., Hofer, L. J. E., and Anderson, R. B., *J. Amer. Chem. Soc.* **75,** 1442 (1953).
4. Borghard, W. G., and Bennett, C. O., *Ind. Eng. Chem. Prod. Res. Dev.* **18,** 18 (1978).
5. Baird, M. J., Schehl, R. R., Haynes, W. P., and Cobb, J. T., Jr., *Ind. Eng. Chem. Prod. Res. Dev.* **19,** 175 (1980).
6. Jack, K. H., *Proc. R. Soc. (London) Ser. A* **195,** 34 (1948).
7. Jack, K. H., *Acta Crystallogr.* **5,** 404 (1952).
8. Bainbridge, J., Channing, D. A., Whitlow, W. H., and Pendelburry, R. E., *J. Phys. Chem. Solid* **34,** 1579 (1973).
9. Chen, G. M., Jaggi, N. K., Butt, J. B., Yeh, E., and Schwartz, L. H., *J. Phys. Chem.* **87,** 5326 (1983).
10. Ron, M., "Application of Mössbauer Spectroscopy." Academic Press, New York, 1980.
11. Niemantsverdriet, J. W., Van Der Kraan, A. M., Van Dijk, W. L., and Van Der Baan, H. S., *J. Phys. Chem.* **84,** 3363 (1980).
12. Amelse, J. A., Arcuri, K. B., Butt, J. B., Matyi, R. J., Schwartz, L. H., and Shapiro, A., *J. Phys. Chem.* **85,** 708 (1981).
13. Barton, G. H., and Gale, B., *Acta Crystallogr.* **17,** 1460 (1964).
14. Matyi, R. J., private communication, Northwestern University, 1982.
15. Shigematsu, T., Bando, Y., and Takada, T., *J. Phys. (Orlay, Fr.)* **40,** C2-153 (1979).
16. A. M., Van Diepen, and Pompa, Th. J.A., *J. Phys. (Orlay, Fr.)* **37,** C6-755 (1976).
17. Amelse, J. A., Ph.D. dissertation, Department of Chemical Engineering, Northwestern University, (1980).
18. LeCaer, G., Dubois, J. M., Pijolat, M., Perrichon, V., and Bussiere, P., *J. Phys. Chem.* **86,** 4799 (1982).
19. Unmuth, E. E., Ph.D. disertation, Department of Chemical Engineering, Northwestern University, (1979).
20. LeCaer, G., Dubois, J. M., and Senateur, J. P., *J. Solid State Chem.* **19,** 19 (1976).
21. Firraro, D., Rosso, M., Principi, G., and Frattini, R., *J. Mater. Sci.* **17,** 1773 (1982).
22. Jack, D. H., and Jack, K. H., *Mater. Sci. Eng.* **11,** 1 (1973).
23. Naumann, F. K., and Langenscheid, G., *Arch. Eisenhuettenwes.* **36,** 677 (1965).
24. Mekata, M., Yoshimura, H., and Takaki, H., *J. Phys. Soc. Jpn.* **33,** 61 (1972).
25. Eickel, K. H., and Pitsch, W., *Phys. Status Solidi* **39,** 121 (1970).
26. DeCristotaro, N., and Kaplow, R., *Metall. Trans. A* **8A,** 425 (1977).
27. Bouchard, R. J., Frederick, C. G., and Johnson, V., *J. Appl. Phys.* **45,** 4067 (1974).
28. Arcuri, K. B., Ph.D. dissertation, Department of Chemical Engineering, Northwestern University (1982).
29. Raupp, G. B., and Delgass, N. N., *J. Catal.* **58,** 337, 348, 361 (1979).
30. Jack, K. H., *J. Iron Steel Inst. London* **169,** 26 (1951).